SAE TECHNICAL PAPER SERIES

2001-01-2742

Experimental and Computational Investigation of Ahmed Body for Ground Vehicle Aerodynamics

Ilhan Bayraktar, Drew Landman and Oktay Baysal
Old Dominion University

SAE The Engineering Society For Advancing Mobility Land Sea Air and Space® INTERNATIONAL

International Truck and Bus Meeting and Exhibition
Chicago, Illinois
November 12-14, 2001

400 Commonwealth Drive, Warrendale, PA 15096-0001 U.S.A. Tel: (724) 776-4841 Fax: (724) 776-5760

ISSN 0148-7191

Printed in USA

2001-01-2742

Experimental and Computational Investigation of Ahmed Body for Ground Vehicle Aerodynamics

Ilhan Bayraktar, Drew Landman and Oktay Baysal
Old Dominion University

ABSTRACT

External aerodynamics remains one of the major concerns in designing a new generation road vehicle. In the present study, the external aerodynamics of an Ahmed body at a scale and Reynolds number, that are representative of a car or light truck at highway speeds, is explored. An experimental model test was compared with a computational model using various back angles. In addition, the experiment allowed lift and drag to be measured at yaw angles up to ±15 degrees. Reynolds number effect on drag and lift coefficients was studied and wind averaged drag coefficients were calculated. The numerical calculations used a Reynolds-averaged, unsteady Navier-Stokes formulation. Both experimental and computational results are presented for back angles of 0-, 12.5-, and 25-degrees, then compared with each other and the data available in the literature.

INTRODUCTION

The airflow in and around a ground vehicle in motion may be grouped into the following two broad categories: internal and external. The *external* flow includes the underbody flow, flow over the body surface, and the wake behind the vehicle. The external flow is typically responsible for about 85% of the drag force on a bluff body. Both the external and the internal flows are highly turbulent, dominated by large separation regions, large and small vortices, and complex recirculation regions. Due to one or more of the aforementioned factors, some of these flows are also unsteady. Therefore, it is desirable to develop the necessary computational tools and benchmark their results with carefully designed experiments. Further, the experimental setups are necessary in determining the aerodynamic forces on the selected prototypes. The facilities for the measurements also need to establish their levels of accuracy by comparing their data with computational results.

Investigation of bluff-body aerodynamics for ground vehicles has started decades ago. The Ahmed body [1] and Morel body [2] are the first published parametric studies, which have been done with a generic car-like body. They measured time averaged force coefficients and showed flow patterns behind the body for different back angles. Recently, these models have been investigated [3, 4] using time averaged computational fluid dynamics (CFD) methods. More recently, there were several studies [5-7] that have been published on unsteady flows behind such bodies.

The present investigation looks at the problem and studies the Ahmed body for real-life conditions. What differs from the previous studies is that the yaw angle and Reynolds number have been added to the problem variables. In addition, an experimental model was built at the true size of a real car, and therefore it was possible to conduct this study at a wide-range Reynolds numbers. Thus, the present work compares full-scale experimental testing and the numerical simulation of a car-like bluff body. Contributions to the field also include the full-scale model simulation and numerical computations.

METHODS

Methodologies for the present wind tunnel tests and the computational fluid dynamics studies will be presented next.

WIND TUNNEL EXPERIMENTS

An Ahmed body [1] has been modeled experimentally at a true automotive scale in order to avoid well-known Reynolds number effect, such as varying separation points. Surface pressures and drag forces at full scale Reynolds numbers were measured for three different back angles; 0-deg, 12.5-deg, and 25-deg. Pressures were measured on the centerline of the four sides and over the entire surface of the nose and the base regions.

Old Dominion University (ODU), working under a Memorandum of Agreement with NASA Langley Research Center, operates the Langley Full-Scale Tunnel [8, 9]. This facility is the second largest in the United States in terms of test section size and is the largest university-run wind tunnel in the world. The open jet test section is semi-elliptical in cross section with a width of 18.29 m (60 ft) and a height of 9.14 m (30 ft). The ground board is 13 m (42.5 ft) wide by 16 m (52.3 ft) long and features a turntable with a diameter of 8.7 m (28.5 ft) Vehicle drag and individual wheel down force can be measured using the current automobile balance.

The ground board is freestanding, such that, a new boundary layer begins at the leading edge with flow both over and under the planar surface. A boundary layer control suction slot was used for all runs to reduce the displacement thickness at the center of the model to about 0.5 inches. The ground board is shown to scale in Figure 1 with the outline of the model.

The Ahmed body model measures 4.91x1.83x1.35 m, representative of a life-size automobile or light truck. It is 4.7 times larger than the model that was used in the original study by Ahmed [1]. The frontal area to test section area ratio is about 1.4%, representing a very small blockage [10]. The modular model design revolves around a light steel space frame with sheet metal panel covering (Figure 2). The free jet and relatively nonexistent blockage make for a very low level of experimental uncertainty. The model was mounted on faired stands, as shown in Figure 3a, at a height of 0.83 m above the ground board.

Pressures were measured with a Pressure Systems Inc. model 8400, 10-inch water column, electronic-scanning module. The estimated uncertainty in the pressure coefficient is ± 0.005. The drag was measured using the aforementioned automotive balance and has an estimated absolute uncertainty of ± 0.003 [9].

COMPUTATIONAL FLUID DYNAMICS

The computer simulation of such a flow field requires solving its governing equations. First, the computer-aided-design (CAD) model of the vehicle-like-body was developed (Figure 2b). Then, a hybrid unstructured mesh, consisting of prismatic and tetrahedral cells, was generated for the computational domain (Figure 3b). The details of the computer code are given in [11], and its implementation for ground vehicle aerodynamics is given in [5, 12].

Since the flowfield being considered herein is in ground proximity and can be unsteady, it requires time-accurate solutions of the viscous-flow equations. Therefore, the set of equations solved for the present study are the time-dependent, Reynolds-averaged, Navier-Stokes equations in their conservative form. Reynolds-averaged quantities are obtained through a time-averaging process. To achieve these simulations within the currently available computer resources and the project milestones, the effects of turbulence needed to be “modeled.” It was realized, however, that none of the existing turbulence models was developed for unsteady flows. Therefore, the present time-accurate, finite-volume CFD methodology with its RNG k-ε turbulence model was previously benchmarked using a series of well-documented flows [3, 5]. Iterative solvers, such as, the incomplete lower upper (ILU) factorization technique used herein, by themselves tend to rapidly decrease in performance as the number of computational mesh elements increases, or if there are large element aspect ratios present. Therefore, the performance of the solver was greatly improved by employing a multigrid technique.

RESULTS AND DISCUSSION

The critical design parameter for the wake flow is known to be the back angle α. Consequently, three different α values (0-deg, 12.5-deg, 25-deg) and six different Reynolds numbers (2.2 M to 13.2M) were chosen for the experiments (Table 1). This wide range of Reynolds number measurements also allowed us to be able to compare with both previous low Reynolds number studies [1, 2] and full scale car or light truck cases [8, 9].

Shown in Figure 4 is the dependency of the drag and lift coefficients on the Reynolds number. In general, drag coefficient decreases and lift coefficient stays relatively constant with Reynolds number. As Reynolds number ranges from 2.2M to 13.2M, C_D differs up to 3.5%. The C_L variation in this range stays within 2.0% except for the 0-deg back-angle case. The lift coefficient for the 0-deg case changes almost 50% within the same range.

In order to calculate the wind-averaged drag coefficients, measurements have been repeated at several yaw angles (0-deg, ±3-deg, ±6-deg, ±9-deg, ±12-deg, ±15-deg). Given below is the formula to obtain the wind-averaged drag, where the arguments of the terms on the right hand side indicate the yaw angle for that particular drag value.

$$\begin{aligned} C_{D,ave} &= 0.219C_D(0) + 0.185(C_D(+3) + C_D(-3)) \\ &+ 0.110(C_D(+6) + C_D(-6)) + 0.078(C_D(+12) \\ &+ C_D(-12)) + 0.022(C_D(+15) + C_D(-15)) \end{aligned}$$

Figure 5 shows the variation of the drag and lift coefficients versus the yaw angle. The wind averaged drag coefficients provide a true measure of vehicle performance under road conditions found in nature [10]. When comparing the drag values of the three back angle configurations in Figure 5 they appear to be consistent in that the difference in C_D between cases at zero-yaw is closely matched by the difference in wind-averaged drag results. One interesting feature is the asymmetry found in the 12.5° back angle case. The difference between right and left yaw measurements may indicate flow hysteresis. Flow that is separated from the body at –15° may not become attached over the same area as the body is yawed through +15° under continuous flow conditions in the wind tunnel. This effect is of course common in airfoil testing as an airfoil’s angle-of-attack is increased beyond stall and then decreased back to a value where flow was previously attached [13]. The influence of the trailing vortex system may also play a role in the flow physics.

The size of the computational domain (Figure 3b) was determined after several test runs with outer bounds at varying distances. Although the shape is symmetric with respect to its longitudinal center plane and the oncoming flow is at zero yaw, by virtue of the shape bluffness and the blunt base, the flow is expected to develop some asymmetry. To determine the extent of asymmetry, computations were performed for both full-body and half-body geometries. The asymmetry detected via the base pressure coefficients was deemed small [5]. Despite this finding, all unsteady computations were performed on the full body configuration.

To study the attainment of mesh independence, several cases were run with sequentially refined meshes. Presented in Figure 6 are the drag coefficients computed on these meshes, the value measured in the wind tunnel and the discrepancy between the computed and measured values. Based on this study, the mesh employed for the cases presented herein had 150x70x60 cells on the body and the total mesh contained about 5.4 million cells. The final mesh was also adapted to the flow in order to improve the computational accuracy. All the computations were performed in parallel mode on the 64-processor SUN HPC 10000 multiprocessor computer of Old Dominion University. For the computational study, six cases based on different values of the back angle α (0-deg, 5-deg, 15-deg, 20-deg, 25-deg and 30-deg) have been considered.

Presented in Figure 7 are the instantaneous pressure coefficient values on the top surface of the body at its symmetry plane. Although the values for different back angles collapse on each other during the expansion followed by the recompression near the front, the rates of the second expansion and their recovery vastly differ. These results indicate very similar trends to those reported in [1]. Further, the present computational and experimental results agree with each other fairly well. The instantaneous force coefficients from the computations and the measurements were also time averaged and plotted in Figure 8. As expected, the lift increases with the increasing back angle almost linearly. However, the drag is fairly insensitive to the back angle changes except when it is at 30-deg. The present measurements again agree pretty well with the present computations as well as the data from ref. [1].

Although six cases with different back angles were computed, for brevity, only the cases with back angles of 0-deg and 25-deg are presented herein via their instantaneous pressure contours at 0.01 sec. intervals (Figure 9). Among the salient features of the flow is the clearly visible shedding of the wake vortices. The shedding from the upper and lower corners is non-symmetric due to the effect of the ground. Further, the shear layer emanating from the lower corner is weaker by the presence of the ground, which in turn weakens the vorticity concentration. The instantaneous velocity streamlines around the body at t = 0.23 sec. for 0-deg back angle and Re=4.4 M flow are presented in Figure 10. The formation of a very formidable wake is now visualized in three dimensions. Another visualization is presented in Figure 11, from both the experiments and the computations, for the top surface. The flowfield is fairly uniform on the top surface.

A time history of the unsteady forces on the body is generated during a time-accurate computational run. These forces, shown in Figure 12, are then analyzed in the frequency domain. The power spectral density from the case with 0-deg back angle and Re = 4.4M, is presented in Figure 13 for the lift, drag, and side forces. The dominant frequencies can then be used to calculate the Strouhal numbers,

$$St = \frac{f.H}{U}$$

where H is the body height and U is the flow speed. The Strouhal numbers for the lift and the side force for the case in Figure 13 are calculated to be 0.106 and 0.086, respectively. To provide some reference values, the values from [6] and [14] will be considered. The Strouhal number reported in [6] for a similar flow but computed from its pressure fluctuations is 0.070. . The Strouhal numbers reported in [14], again for a similar flow but computed from its trapped vortices and trailing vortices, were 0.073 and 0.110, respectively. Therefore, the present values can be deemed in qualitative agreement with these reported results.

CONCLUDING REMARKS

The external aerodynamics of an Ahmed body was studied with full-scale wind tunnel experiments and by solving the time-dependent, three-dimensional, Reynolds-averaged Navier Stokes equations.

The unsteady flowfield was presented using computational flow visualization. Reynolds number dependency was also investigated, and wind averaged drag coefficients were calculated for each of the experimental cases. The results from both experimental and computational methods were presented for different back angles and compared with each other. The variation of the lift force with the back angle was demonstrated.

REFERENCES

1. Ahmed, S. R., Ramm, G., Faltin, G., 1984, "Some Salient Features of the Time-Averaged Ground Vehicle Wake," SAE Paper 840300, SAE International Congress, Detroit, MI.
2. Morel, T., 1978, "Aerodynamic Drag of Bluff Body Shapes Characteristic of Hatch-Back Cars", SAE Paper 780267.
3. Han, T., 1989, "Computational Analysis of Three-Dimensional Turbulent Flow Around a Bluff Body in Ground Proximity," AIAA Journal, 27, No. 9, pp.1213-1219.
4. Anagnost, A., Alajbegovic, A., Chen, H., Hill, D., Teixeira, C., Molving, K., 1997, "Digital Physics Analysis of Morel Body in Ground Proximity", SAE Paper 970139.
5. Baysal, O., and Bayraktar, I., 2001, "Unsteady Wake Behind a Bluff Body in Ground Proximity", FEDSM2001-18208, ASME Fluids Engineering Division Summer Meeting, New Orleans, LA.
6. Khalighi, B., Zhang, S., Koromilas, C., Balkanyi, S., Bernal, L., Iaccarino, G., Moin, P., 2001, "Experimental and Computational Study of Unsteady Wake Flow behind a Bluff Body with a Drag Reduction Device", SAE Paper 2001-01-1042, SAE World Congress, Detroit, MI.
7. Krajnovic, S., Davidson, L., 2001, "Large-Eddy Simulation of the Flow Around a Ground Vehicle Body", SAE Paper 2001-01-0702, SAE World Congress, Detroit, MI.
8. Landman, D., 2000, "Road Simulation for NASCAR Vehicles at the Langley Full-Scale Tunnel," SAE 00MSV-31.
9. Landman, D. and Britcher, C. P., 1998, "Development of Race Car Testing at the Langley Full-Scale Tunnel," SAE 98MSV-21.
10. Hucho, W. H., 1998, Aerodynamics of Road Vehicles, SAE Publishing, Warrendale, PA.
11. CFX-5 Solver and Solver Manager, 1999, AEA Technologies, Pittsburgh, PA.
12. Baysal, O., and Bayraktar, I., 2000, "Computational Simulations for the External Aerodynamics of Heavy Trucks" SAE Paper 2000-01-3501, International Truck and Bus Meeting& Exposition, Portland, OR.
13. Abbott, I.H. and Von Doenhoff, A.E., 1959, Theory of Wing Sections, Dover Publishers, New York, NY.
14. Krajnovic, S. and Davidson, L., 2001, "Large-Eddy Simulation of the Flow Around a Ground Vehicle Body", SAE Paper 2001-01-0702, SAE World Congress, Detroit, MI.

CONTACTS

Oktay Baysal, PhD, PE
Professor, Eminent Scholar, and Associate Dean
College of Engineering and Technology
Old Dominion University
Norfolk, VA 23529-0236
Phone: (757) 683 3789 Fax: (757) 683 4898
e-mail: obaysal@odu.edu
web: www.eng.odu.edu/baysal

and

Drew Landman, PhD, PE
Chief Engineer
Langley Full-Scale Tunnel
P.O. Box 65309
Langley AFB, VA 23665-5309
Phone: (757) 766 2266 Fax: (757) 766 3104
e-mail: dlandman@odu.edu

Table. 1. Experimental measurements for test cases with varying back angle, yaw angle and Reynolds number (Re number in millions: i=2.2M, ii=4.4M, iii=8.8M, iv=13.2M).

Back angle \ Yaw angle	0-deg	±3-deg	±6-deg	±9-deg	±12-deg	±15-deg
0.0-deg	i,ii,iii,iv	i,ii,iii,iv	iii	iii	iii	iii
12.5-deg	ii,iii,iv	ii,iii,iv	iii	iii	iii	iii
25.0-deg	ii,iii,iv	ii,iii,iv	ii,iii	ii,iii	ii,iii	ii,iii

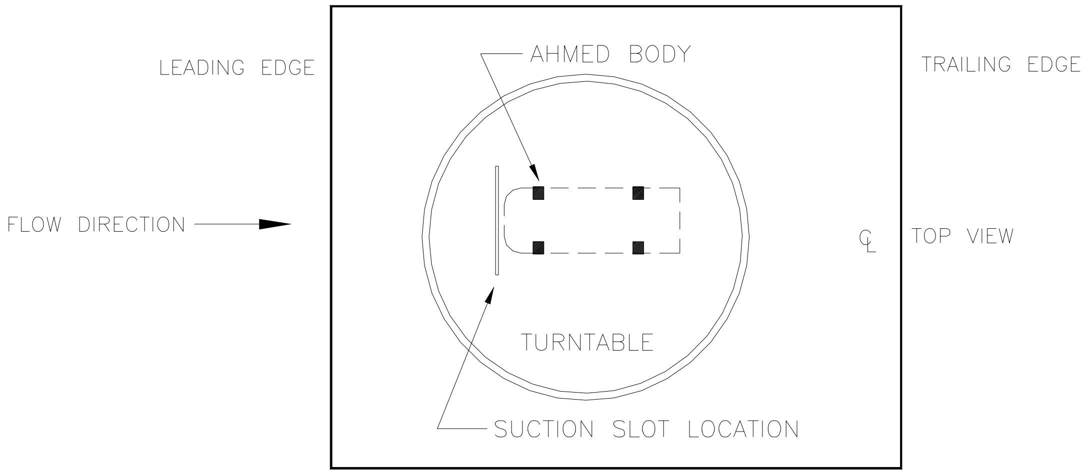

Figure 1. The ground board in the test section of Langley Full Scale Tunnel [8].

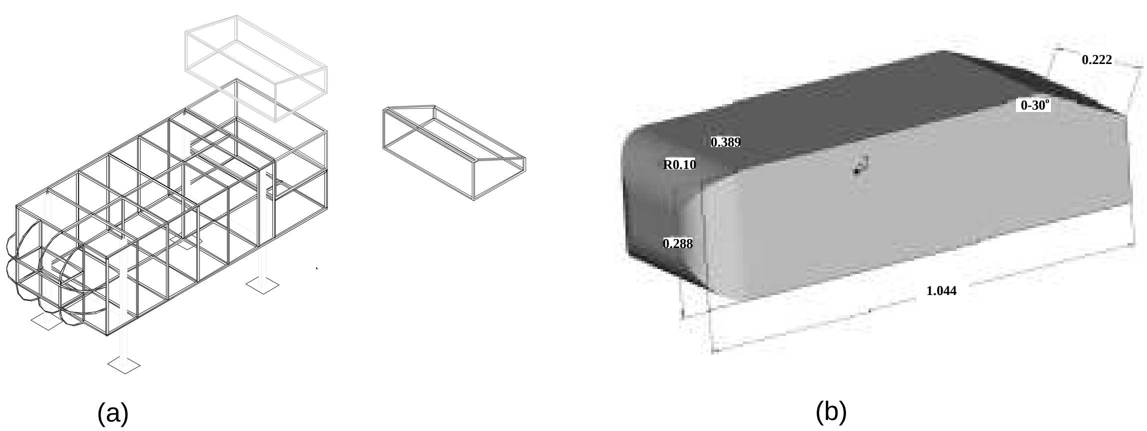

Figure 2. Ahmed body. (a) Experimental model and its back panels, (b) Computational model (all units in meters).

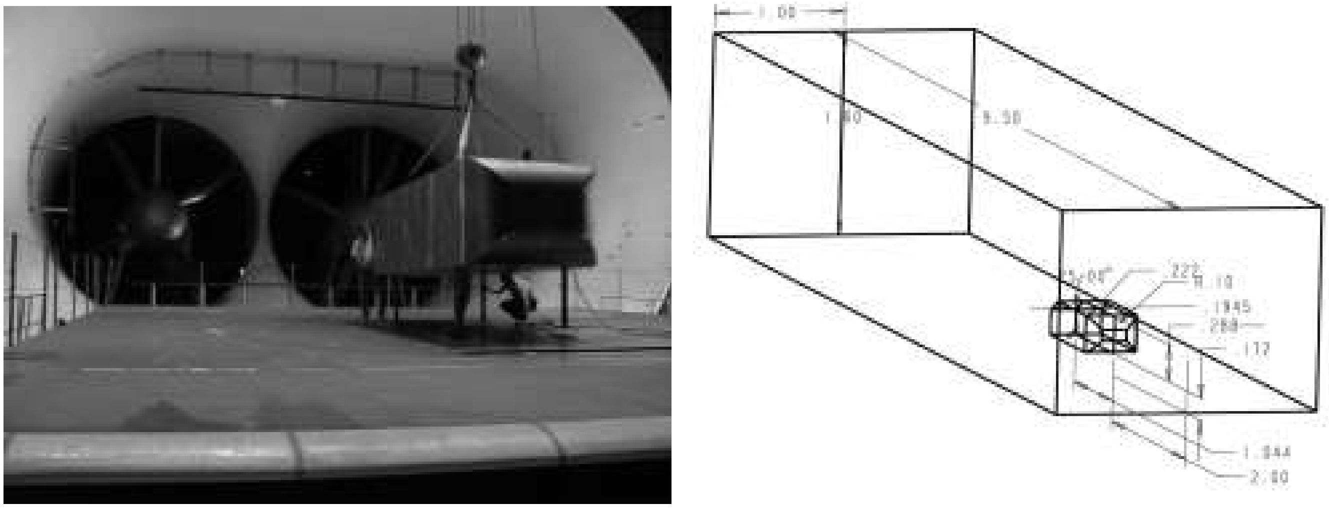

(a) (b)

Figure 3. Experimental set up and the computational domain (all units in meters).

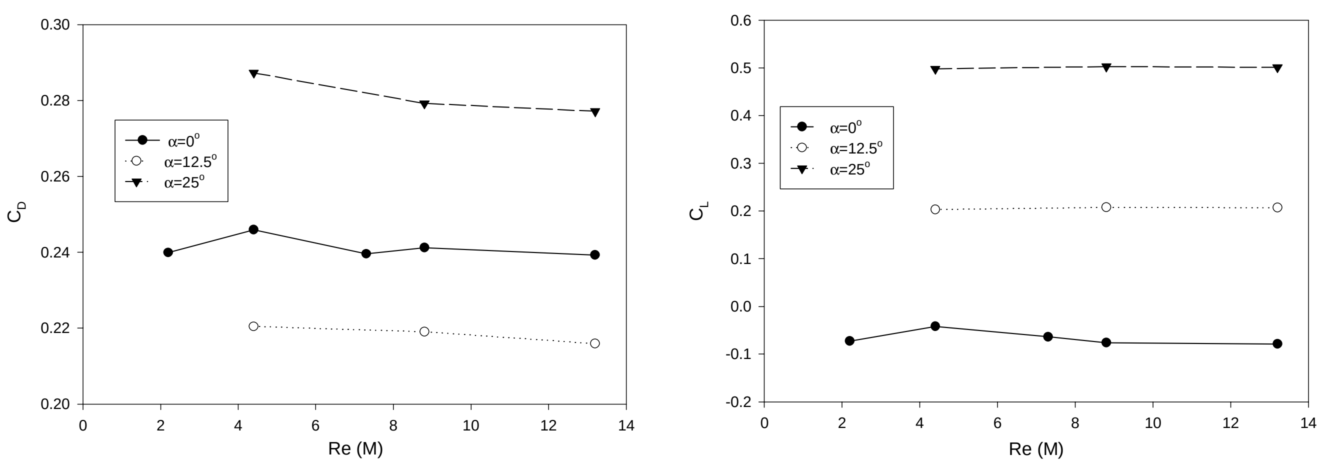

Figure 4. Effect of varying the flow Reynolds number on drag and lift coefficients (zero yaw angle).

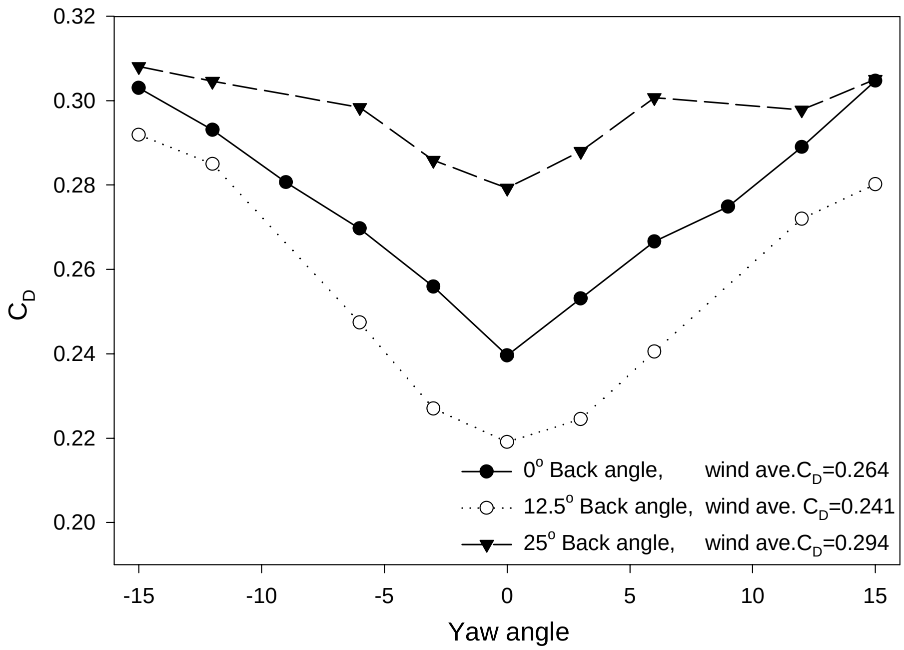

Figure 5. Wind-averaged drag coefficients for bodies with three different back angles (Re=8.8M).

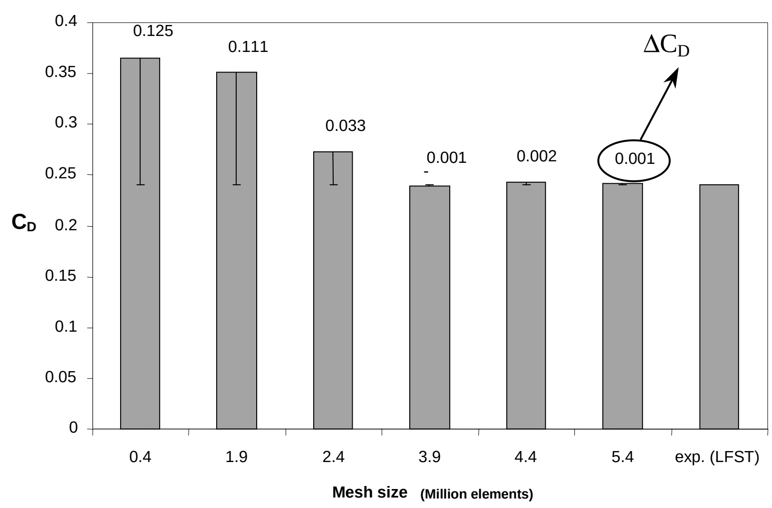

Figure 6. Improvement in drag computations by increasing mesh density and their comparison with wind-tunnel measurements (0-deg. back angle, Re=4.4 M).

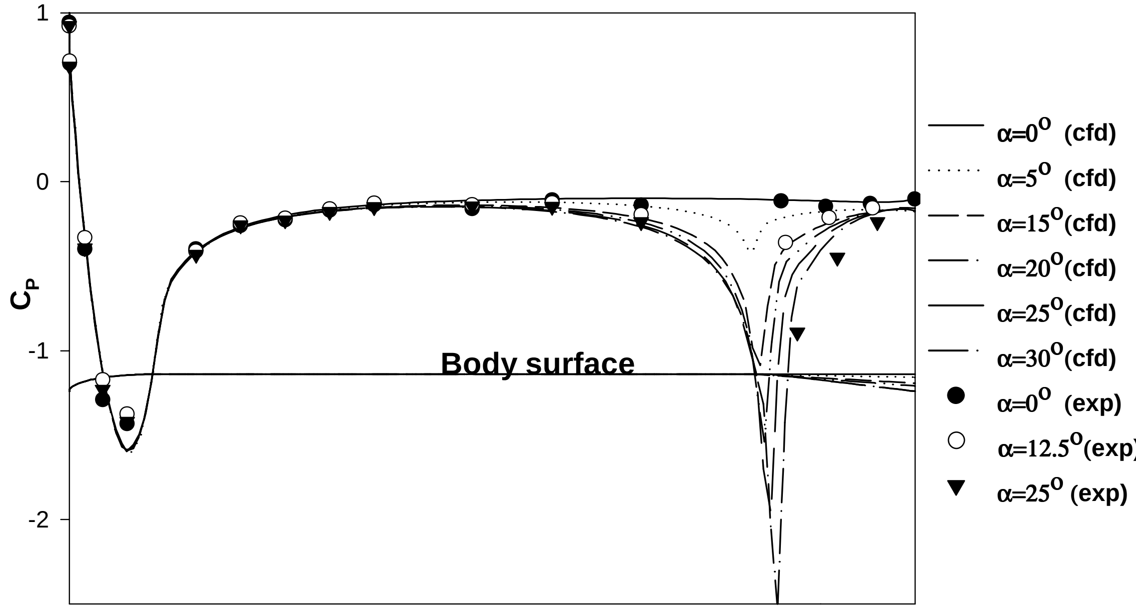

Figure 7. Experimental (exp) and computational (CFD) pressure coefficient distributions on the top surface at body symmetry plane for various back angles.

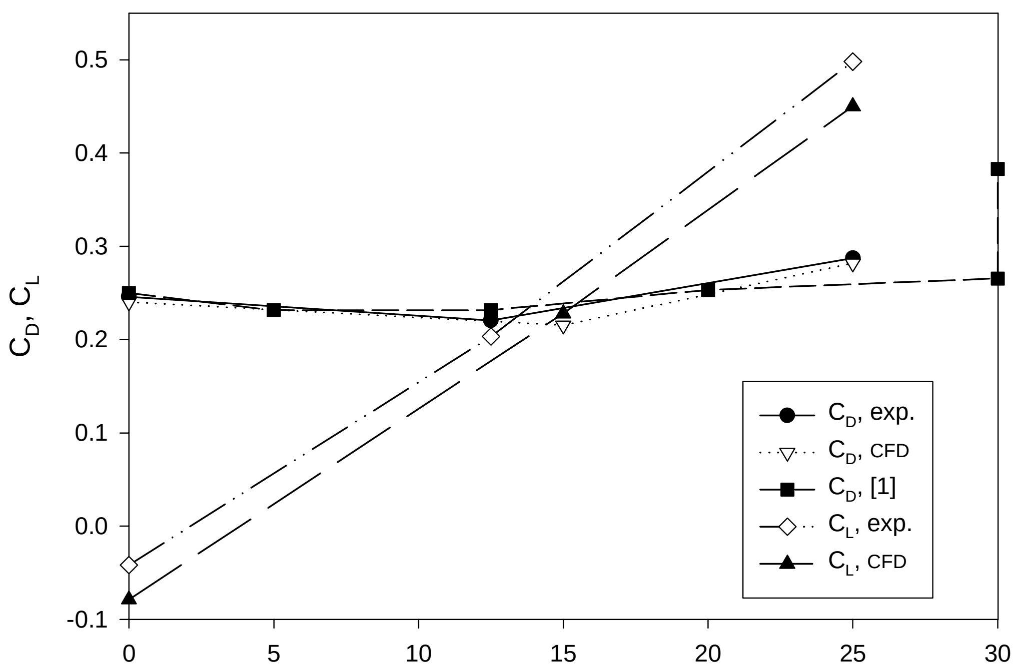

Figure 8. Comparisons of time-averaged drag and lift coefficients from present computational and experimental (exp) studies and the experimental data from ref. [1] (Re=4.4M).

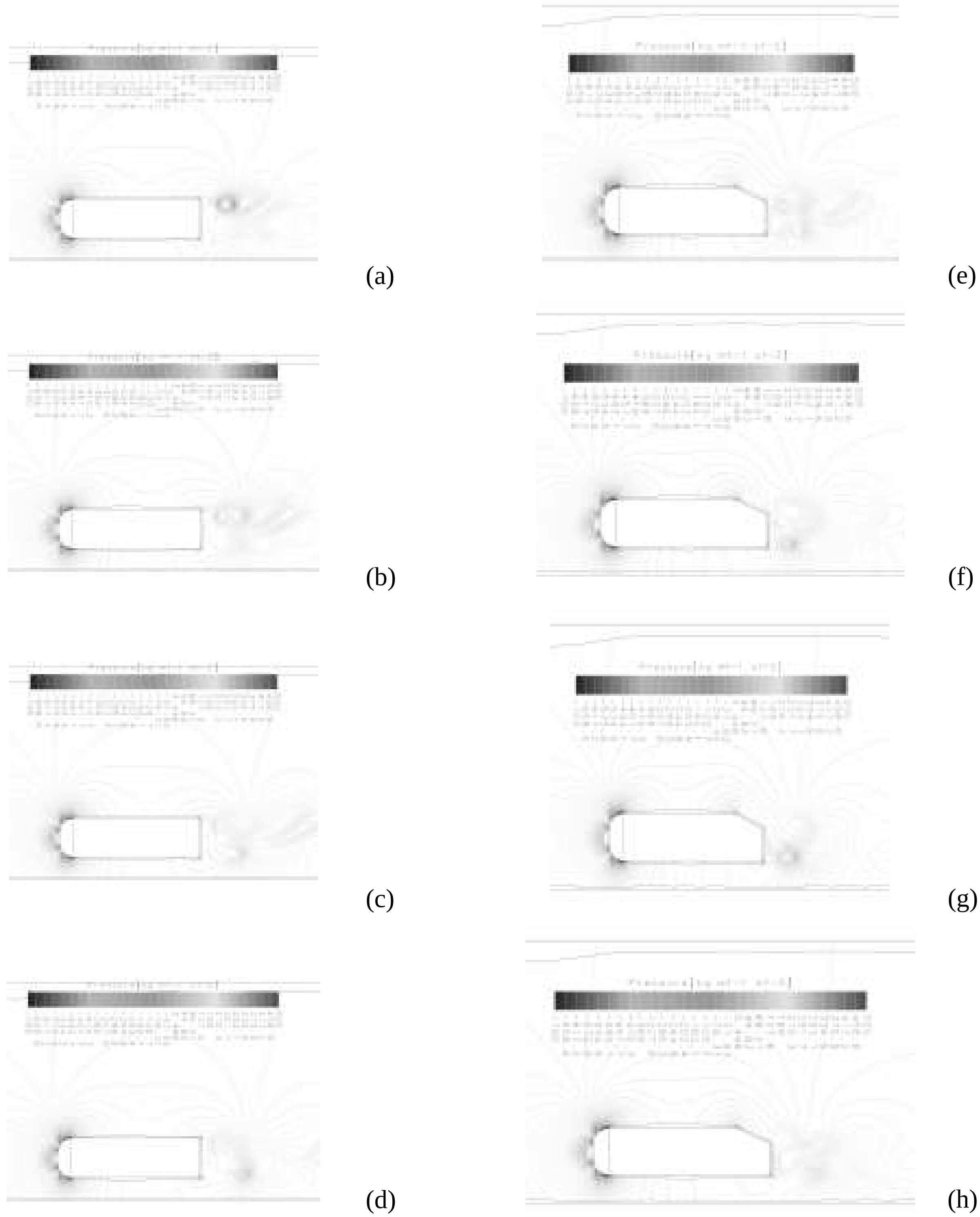

Figure 9. Computed instantaneous pressure contours of the longitudinal symmetry plane at t = 0.20, 0.21, 0.22, and 0.23 sec. (a)-(d) α=0°, (e)-(h) α=25°.

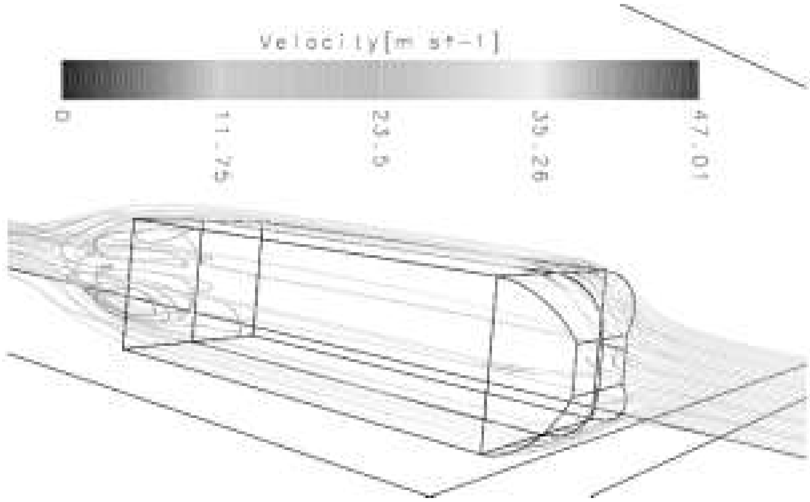

Figure 10. Computed instantaneous velocity streamlines at t=6.3050 sec. (0-deg back angle, Re=4.4 M)

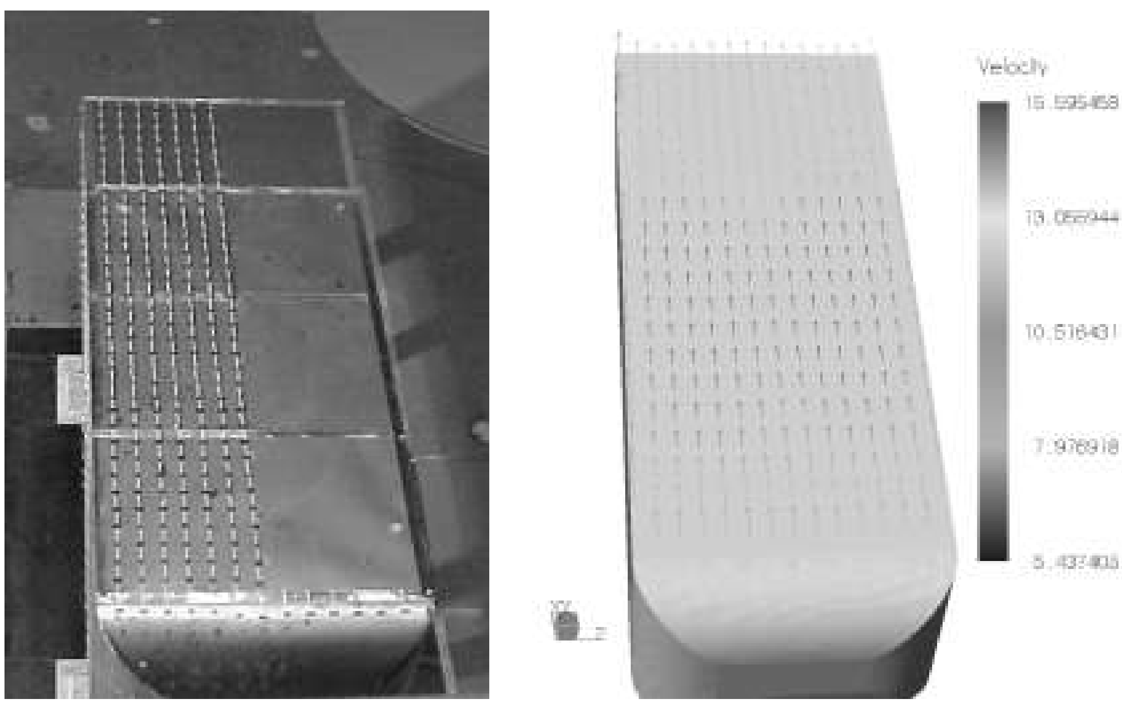

Figure 11. Tuft visualization from the wind tunnel and computed instantaneous vector plots on the top surface (0-deg back angle, Re=8.8M).

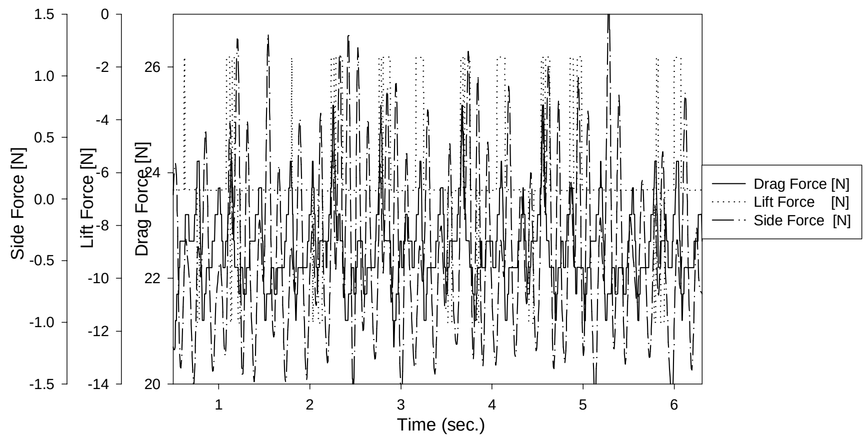

Figure 12. Time variation of force components on the body (0-deg back angle, Re=4.4 M)

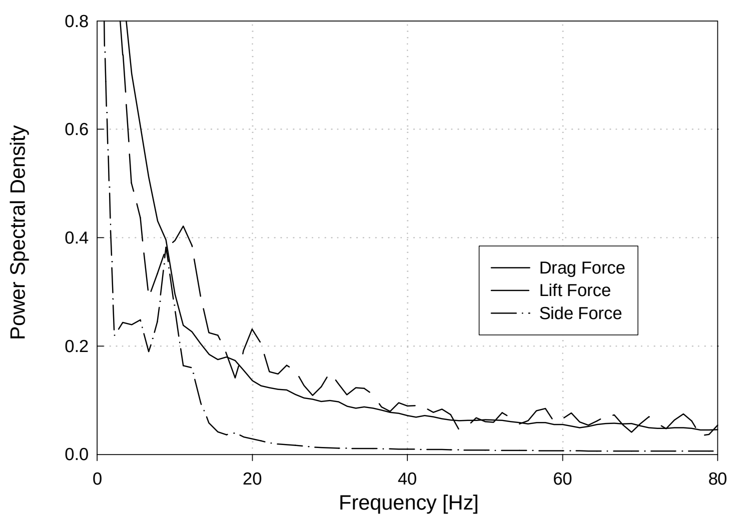

Figure 13. Power spectral density variation on the force data (0-deg back angle, Re=4.4 M).